Dynamics of Track/Wheel Systems on High-Speed Vehicles

Isamu Kato
Department of Mechanical Engineering, Sophia University, 7-1 Kioi-cho, Chiyoda-ku, Tokyo 102-8554, Japan
Yoshiaki Terumichi*
Department of Mechanical Engineering, Sophia University, 7-1 Kioi-cho, Chiyoda-ku, Tokyo 102-8554, Japan
Masahito Adachi
Technology Research and Development Department, Central Japan Railway Company, 1545-33, Oyama, Komaki-shi, Aichi 485-0801, Japan
Kiyoshi Sogabe
Department of Mechanical Engineering, Sophia University, 7-1 Kioi-cho, Chiyoda-ku, Tokyo 102-8554, Japan

For high speed railway vehicles, we consider a vibration of flexible track/wheel system. It is very important to deal with the complex phenomena of high-speed vehicles that can be occurred in the vertical vibration of the system. From a viewpoint of multibody dynamics, this kind of problem needs accurate analysis because the system includes mutual dynamic behaviors of rigid body and flexible body. The simulation technique for the complex problems is also discussed. We consider the high-speed translation, rail elasticity, elastic supports under the rail and contact rigidity. Eigen value analysis is also completed to verify the mechanism of the coupled vertical vibration of the system.

Key Words : Contact, Flexible Multibody Dynamics, Absolute Nodal Coordinate Formulation, Railroad Systems

Nomenclature

A : Center of a wheel
B : Contact point on a rail
Q : Contact point on a wheel
O-XY : Absolute coordinate
A-X_AY_A : Moving frame fixed for a center of a wheel.
B-X_BY_B : Moving frame fixed for a contact point.
k : Rate of contact rigidity
θ : Rotation angle of the wheel
ϕ : Obliquity of a rail
s : Coordinate along rail
$\rho(t)$: Distance between a wheel center and a rail
d : Distance of elastic supports
k_s : Rate of elastic supports

* Corresponding Author,
E-mail : y-terumi@sophia.ac.jp
TEL : +81-3-3238-3314; **FAX** : +82-3-3238-3311
Department of Mechanical Engineering, Sophia University, 7-1 Kioi-cho, Chiyoda-ku, Tokyo 102-8554, Japan. (Manuscript **Received** November 29, 2004; **Revised** December 15, 2004)

1. Introduction

This paper deals with modeling and numerical simulation for dynamic behavior of track/wheel systems on high-speed vehicles, considering an elastic rail, a flexible track and rolling wheels. Numerical method for the accurate solution is also discussed, considering its high-speed translation. It is assumed that the motion of the system is restricted in plane.

Considering the vibration problem of the high-speed railway system, it is important to analyze

the mutual dynamic behavior of the system between the wheel-motion and the track-motion with the unilateral contact. When the vehicle runs with high-speed, the complex phenomena in the vertical vibration of the system occur, and so it is also important to cope with the simulation technique considering high-speed translation. The translation speed is not negligible compared with the propagation speed of vibration wave. The frequency of the passage through the elastic support of the track is not so low. Then it is expected that the interaction between the vertical vibration and the translation influences on the system behavior. It is required that the simulation technique for such like problems is developed and it causes great contribution to the design for the practical systems.

In this paper, a rolling disk and an elastic beam with elastic supports are modeled as the rail/wheel system. In order to analyze the motion of elastic rail, the Absolute Nodal Coordinate Formulation, Shabana (1998) is applied. The contact position between the rolling wheel and the rail gives the constraint condition for the unilateral contact. Elastic supports underneath elastic rail and the contact rigidity between the rolling wheel and the elastic rail are also taken into account. The dynamic load on the rail is caused due to the interaction of these elements.

Eigen value analysis is also attempted. This system raises the coupled motion between the concentrated system and the flexible system, which is due to the elastic rail, the rolling wheel and the flexible track. The natural frequency of the system depends on the position of the wheel on the elastic rail on the flexible track. Some numerical results for the motion of the system during the passage of the wheel on the flexible track are discussed. It is clarified how high-speed translation influences on the system vibration.

2. Modeling and Formulation

In this paper, we consider a rolling wheel on an elastic rail with elastic supports as rail/wheel system. The model for the wheel rolling on the flexible track is shown in Fig. 1. The elastic

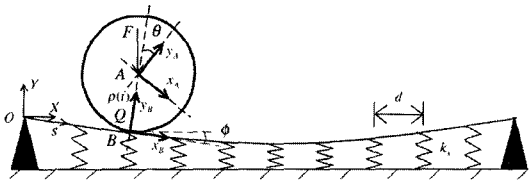

Fig. 1 Analytical model

rail is modeled as a flexible beam that is simple supported at the both ends. We describe the flexible beam motion by using the Absolute Nodal Coordinate Formulation, Shabana (1998), Takahashi and Shimizu (2001). The rolling wheels and the flexible beam contact at a point each other with contact rigidity that is derived from Hertz's theory, Terumichi (2001). We also consider slip between the wheel and the rail. In this chapter, modeling for a wheel that rolls on the flexible rail is developed because it is supposed that the wave propagation speed in the rail cannot be negligible for high-speed translation. The formulation of the system of the flexible rail/wheel system is completed, considering the slip, contact rigidity, support stiffness, rail elasticity.

2.1 Unilateral contact between elastic rail and wheel

The simple model for a rolling wheel on the flexible track is shown in Fig. 2.

O-XY coordinate is the fixed frame with an orthogonal set. A-x_Ay_A coordinate whose origin is fixed on the center of the wheel and it moves and rotates with the wheel. B-x_By_B coordinate is fixed on the contact point and moves with its translation. We also introduce s that is the coordinate along the rail and function of time t. Due to its dynamic behavior, the obliquity ϕ of the rail is function of $s(t)$ for the translation of the wheel and also the function of time t for the vibration of the elastic rail as

$$\phi=\phi(s(t),\ t) \tag{1}$$

B denotes the contact point between the wheel and the rail and is on the rail. On the other hand, Q denotes the contact point between the wheel and the rail and is fixed on the wheel. The

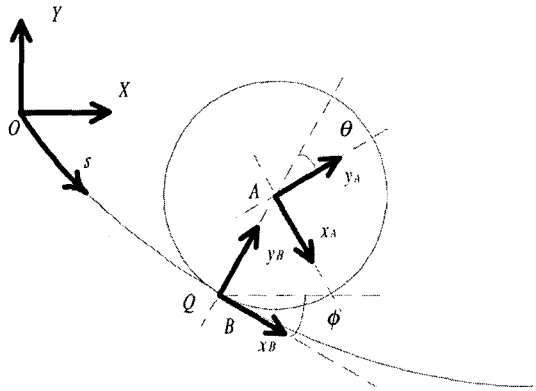

Fig. 2 Model of a wheel on the rail

position vector $\mathbf{r}_{OB}$ can be revealed in the fixed frame O-XY as follows;

$$\mathbf{r}_{OB}=\mathbf{R}_{OA}-\mathbf{C}_{OB}\mathbf{e}_{y_B}\rho \tag{2}$$

where ρ is the distance between the contact point and the wheel center.

Considering the obliquity ϕ, the differentiation of the transformation matrix $\mathbf{C}_{OB}$ can be derived as

$$\begin{aligned}\frac{d}{dt}\mathbf{C}_{OB}&=\dot{\phi}\mathbf{c}^R_{OB}\mathbf{C}_{OB}+\frac{ds}{dt}\frac{\partial\phi}{\partial s}\mathbf{c}^R_{OB}\mathbf{C}_{OB}\\&=\dot{\phi}\mathbf{c}^R_{OB}\mathbf{C}_{OB}+\mathbf{v}_s\frac{\partial\phi}{\partial s}\mathbf{c}^R_{OB}\mathbf{C}_{OB}\end{aligned} \tag{3}$$

The velocity vector $\mathbf{v}_{OB}$ can be expressed base on this as

$$\mathbf{v}_{OB}=\frac{d}{dt}\mathbf{R}_{OA}-\frac{d}{dt}\mathbf{C}_{OB}\mathbf{e}_{y_B}\rho-\mathbf{C}_{OB}\mathbf{e}_{y_B}\frac{d}{dt}\rho \tag{4}$$

The position vector $\mathbf{r}_{OQ}$ can be written in the fixed frame O-XY as follows;

$$\mathbf{r}_{OQ}=\mathbf{R}_{OA}+\mathbf{C}_{OA}\mathbf{r}'_{AQ} \tag{5}$$

where $\mathbf{r}'_{AQ}$ is the position vector to the contact point Q from the origin of the local frame A-X_AY_A that is also the center of the wheel, and can be written as

$$\mathbf{r}_{AQ}=-\mathbf{C}^T_{OA}\mathbf{C}_{OB}\mathbf{e}_{y_B}\rho \tag{6}$$

Differentiation of Equation (6) with respect to the time can be written using Equation (3) as

$$\begin{aligned}\dot{\mathbf{r}}_{AQ}&=\mathbf{C}^T_{OA}\frac{d}{dt}\mathbf{C}_{OB}\mathbf{e}_{y_B}-\mathbf{C}^T_{OA}\mathbf{C}_{OB}\mathbf{e}_{y_B}\frac{d}{dt}\rho\\&=-\mathbf{C}^T_{OA}\left(\dot{\phi}\mathbf{c}^R_{OB}\mathbf{C}_{OB}+\mathbf{v}_s\frac{\partial\phi}{\partial s}\mathbf{c}^R_{OB}\mathbf{C}_{OB}\right)\mathbf{e}_{y_B}\rho-\mathbf{C}^T\mathbf{C}_{OB}\mathbf{e}_{y_B}\dot{\rho}\end{aligned} \tag{7}$$

By differentiating Equation (5), the velocity vector of the contact point $\boldsymbol{Q}$ can be derived as

$$\mathbf{v}_{OQ}=\mathbf{v}_{OA}+\dot{\mathbf{C}}_{OA}\mathbf{r}_{AQ}+\mathbf{C}_{OA}\dot{\mathbf{r}}_{AQ} \tag{8}$$

From Equations (6), (7), and (8), we obtain the following equation.

$$\begin{aligned}\mathbf{v}_{OQ}=\mathbf{V}_{OA}&-\dot{\theta}\mathbf{C}_{OB}\mathbf{e}_{x_B}\rho+\dot{\phi}\mathbf{C}_{OB}\mathbf{e}_{x_B}\rho\\&+\mathbf{v}_s\frac{\partial\phi}{\partial s}\mathbf{C}_{OB}\mathbf{e}_{x_B}\rho-\mathbf{C}_{OB}\mathbf{e}_{y_B}\dot{\rho}\end{aligned} \tag{9}$$

The terms in the right hand side are translation velocity of the center of the wheel, rotation velocity of the wheel, the vertical velocity of the contact point due to the rail motion, the velocity caused by rolling wheel on the flexible rail and the velocity due to the contact rigidity in order. Here,

$$\mathbf{C}_{OB}\mathbf{e}_{x_B}=\begin{bmatrix}\cos\phi & -\sin\phi\\ \sin\phi & \cos\phi\end{bmatrix}\begin{bmatrix}1\\0\end{bmatrix}=\begin{bmatrix}\cos\phi\\ \sin\phi\end{bmatrix} \tag{10}$$

$$\mathbf{C}_{OB}\mathbf{e}_{y_B}=\begin{bmatrix}\cos\phi & -\sin\phi\\ \sin\phi & \cos\phi\end{bmatrix}\begin{bmatrix}0\\1\end{bmatrix}=\begin{bmatrix}-\sin\phi\\ \cos\phi\end{bmatrix} \tag{11}$$

Using the above relations Equation (9) can be rewritten as

$$\begin{aligned}\mathbf{v}_{OQ}=\mathbf{V}_{OA}&+\begin{bmatrix}-\rho\cos\phi\\ -\rho\sin\phi\end{bmatrix}\dot{\theta}\\&+\begin{bmatrix}\rho\cos\phi\\ \rho\sin\phi\end{bmatrix}\left(\dot{\phi}+\mathbf{v}_s\frac{\partial\phi}{\partial s}\right)+\begin{bmatrix}\dot{\rho}\sin\phi\\ -\dot{\rho}\cos\phi\end{bmatrix}\end{aligned} \tag{12}$$

Using the shape function $\mathbf{S}$ and the nodal coordinates $\mathbf{e}$ of the A.N.C formulation, the position vector of $\mathbf{r}_{OB}$ at the contact point B on the rail can be written as

$$\mathbf{r}_{OB}=\mathbf{S}\mathbf{e} \tag{13}$$

From this relation, we can lead the velocity vector as

$$\mathbf{v}_{OB}=\mathbf{S}\dot{\mathbf{e}} \tag{14}$$

The constraint of the unilateral contact between the wheel and the rail must be satisfied by the following equation

$$\mathbf{r}_{OQ}=\mathbf{r}_{OB} \tag{15}$$

From Equation (14) and Equation (15), we obtain the following relation.

$$\mathbf{v}_{OQ}=\mathbf{v}_{OB}=\mathbf{S}\dot{\mathbf{e}} \tag{16}$$

Using Equation (12), we can rewrite Equation (16) to the following non-holonomic constraint equation.

$$\begin{aligned}\mathbf{V}_{OA}&+\begin{bmatrix}-\rho\cos\phi\\-\rho\sin\phi\end{bmatrix}\dot{\theta}+\begin{bmatrix}\rho\cos\phi\\\rho\sin\phi\end{bmatrix}\left(\dot{\phi}+\mathbf{v}_s\frac{\partial\phi}{\partial s}\right)\\&+\begin{bmatrix}\dot{\rho}\sin\phi\\-\dot{\rho}\cos\phi\end{bmatrix}-\mathbf{S}\dot{\mathbf{e}}=\mathbf{0}\end{aligned} \tag{17}$$

This equation can be expressed as follows;

$$\Phi_{\mathbf{v}OA}\mathbf{V}_{OA}+\Phi_{\dot{\theta}}\dot{\theta}+\Psi_t=\mathbf{0} \tag{18}$$

where

$$\begin{aligned}\Phi_{\mathbf{v}OA}&=\begin{bmatrix}1&0&0\\0&1&1\end{bmatrix},\ \Phi_{\dot{\theta}}=\begin{bmatrix}-\rho\cos\phi\\-\rho\sin\phi\end{bmatrix}\\\Psi_t&=\begin{bmatrix}\rho\cos\theta\\\rho\sin\phi\end{bmatrix}\left(\dot{\phi}+\mathbf{v}_s\frac{\partial\phi}{\partial s}\right)+\begin{bmatrix}\dot{\rho}\sin\phi\\-\dot{\rho}\cos\phi\end{bmatrix}-\mathbf{S}\dot{\mathbf{e}}\end{aligned} \tag{19}$$

By differentiating Equation (18), we can obtain the equation as

$$\Phi_{\mathbf{v}OA}\dot{\mathbf{V}}_{OA}+\Phi_{\dot{\theta}}\ddot{\theta}+(\dot{\Phi}_{\mathbf{v}OA}\mathbf{V}_{OA}+\dot{\Phi}_{\dot{\theta}}\dot{\theta}+\dot{\Psi}_t)=\mathbf{0} \tag{20}$$

We can rewrite this constraint condition as

$$\begin{aligned}\mathbf{V}_{OA}&+\begin{bmatrix}-\rho\cos\phi\\-\rho\sin\phi\end{bmatrix}\ddot{\theta}+\begin{bmatrix}\rho\sin\phi\\-\rho\cos\phi\end{bmatrix}\dot{\theta}\left(\dot{\phi}+\mathbf{v}_s\frac{\partial\phi}{\partial s}\right)\\&+\begin{bmatrix}-\dot{\rho}\cos\phi\\-\dot{\rho}\sin\phi\end{bmatrix}\dot{\theta}+\begin{bmatrix}\rho\cos\phi\\\rho\sin\phi\end{bmatrix}\left(\ddot{\phi}+\dot{\mathbf{v}}_s\frac{\partial\phi}{\partial s}+\mathbf{v}_s^2\frac{\partial^2\phi}{\partial s^2}+2\mathbf{v}_s\frac{\partial^2\phi}{\partial s\partial t}\right)\\&+\begin{bmatrix}-\rho\sin\phi\\\rho\cos\phi\end{bmatrix}\left(\dot{\phi}+\mathbf{v}_s\frac{\partial\phi}{\partial s}\right)^2+2\begin{bmatrix}\dot{\rho}\cos\phi\\\dot{\rho}\sin\phi\end{bmatrix}\left(\dot{\phi}+\mathbf{v}_s\frac{\partial\phi}{\partial s}\right)\\&+\begin{bmatrix}\ddot{\rho}\sin\phi\\-\ddot{\rho}\cos\phi\end{bmatrix}-\mathbf{S}\ddot{\mathbf{e}}=0\end{aligned} \tag{21}$$

2.2 Differential algebraic equations

Several assumptions about the force transmission are set. External torque $\mathbf{N}_{OA}$ acts at the center of the wheel and external forces $\mathbf{F}_{OA}$ act on the center of the wheel. Using the radius of the wheel without contact ρ_0 and the contact rigidity k, $\mathbf{F}_{OA}$ can be written as

$$\mathbf{F}_{OA}=\begin{bmatrix}\cos\phi&-\sin\phi\\\sin\phi&\cos\phi\end{bmatrix}\begin{bmatrix}0\\-F-Mg-k(\rho-\rho_0)\end{bmatrix} \tag{22}$$

We assume that unknown constraint force and torque $\bar{\mathbf{F}}_{OA}$ and $\bar{\mathbf{N}}_{OA}$ act on the center of the wheel. Considering Equation (22) and these assumptions, we can obtain the equations of wheel motion as follows;

$$\mathbf{M}_A\dot{\mathbf{V}}_{OA}=\mathbf{F}_{OA}+\bar{\mathbf{F}}_{OA} \tag{23}$$

$$\mathbf{J}_{OA}\ddot{\theta}=\mathbf{N}_{OA}+\bar{\mathbf{N}}_{OA} \tag{24}$$

Finally, the differential algebraic motion can be written as

$$\begin{bmatrix}\mathbf{M}_A&0&\Phi_{\mathbf{v}OA}^T\\0&J_{OA}&\Phi_{\dot{\theta}}\\\Phi_{\mathbf{v}OA}&\Phi_{\dot{\theta}}&0\end{bmatrix}\begin{bmatrix}\dot{\mathbf{V}}_{OA}\\\ddot{\theta}\\\Lambda\end{bmatrix}=\begin{bmatrix}\mathbf{F}_{OA}\\N_{OA}\\\gamma\end{bmatrix} \tag{25}$$

The wheel motion and the rail motion are coupled between the contact force and the obliquity of the rail ϕ.

The rail motion equation is follow;

$$\mathbf{M}\ddot{\mathbf{e}}=\mathbf{Q}_f-\mathbf{Q}_{kl}-\mathbf{Q}_{kt}-\mathbf{Q}_s \tag{26}$$

where $\mathbf{Q}_f$ is the external force, $\mathbf{Q}_{kl}$ and $\mathbf{Q}_{kt}$ are elastic forces of the beam and $\mathbf{Q}_s$ is elastic force of the support.

3. Eigen Value Problems

In this chapter, we consider the static condition of the system for eigen value analysis. Mass matrix and stiffness matrix are denoted by F.E.M for linear problem. The system consists of the wheel, the flexible beam and the supports with the spring constant. The contact rigidity is also considered and the wheel is modeled as the linear spring-mass system. The equation of motion is described with the following form.

$$\mathbf{M}\ddot{\mathbf{x}}+\mathbf{K}\mathbf{x}=0 \tag{27}$$

It is assumed that the mass-spring system is located on the nodes set on the beam and the support spring is connected on the nodes. Eigen values and vectors for the above equation are calculated using QZ method.

The eigen values of the system are shown in Fig. 3. In this figure, eigen values are shown to the 4_{th} mode. The lowest one corresponds to the motion of the beam with the wheel as the rigid

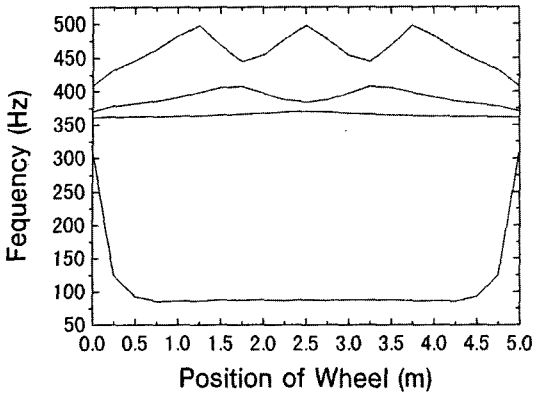

Fig. 3 Eigen values of the system

body. The second one corresponds to the motion of the mass-spring system on the beam. Then, it is almost constant in spite of its location on the beam. Third and fourth ones are due to the beam flexibility. They fluctuate with the mass position due to the effect of the coupled motion between the wheel and the rail. But we can also see the change of the natural frequency of the beam supported at its both ends.

4. Numerical Results

We verify the number of elements and the integration time step for the numerical simulation. Next, we attempt to simulate for the motion of a wheel on flexible rail, changing some parameters such as the moving velocity and the support elasticity. Then, the dynamic behavior of the wheel and the rail are discussed, considering the eigen values.

4.1 Parameters in simulation

In this paper, the following parameters in Table 1 for the wheel/rail systems are used. The shape of the rail is approximated to rectangle. Length of the rail is 5 m and elastic support is placed with the interval of 0.5 m and its spring constant is 140 MN/m. The vertical load 47040 N is given to the center of the wheel as car body weight.

4.2 Element number and time step

The numerical results for the wheel passage on the flexible beam with the integration time step $10^{-6}s$, $10^{-7}s$ and $10^{-8}s$ are shown in Fig. 4. The moving velocity, 50 km/h, the support elasticity 140 MN/m and the number of elements 20 are given. In this result, according to the judgment of slip, it is mentioned that the wheel moves without slip and so the translation velocity coincides with the rotation velocity. Then calculation error v_e can be defined as

$$v_e=\frac{\dot{x}-\rho\dot{\theta}}{\dot{x}}\times 100 \tag{28}$$

From these results, the calculation error and the displacement of the contact point with the integration time step $10^{-6}s$, $10^{-7}s$ and $10^{-8}s$ are in good agreement quantitatively. Integration time step $10^{-6}s$ is also sufficient to estimate the displacement of the contact point. However, we need $10^{-7}s$ to discuss about its acceleration. In addition, we also cannot calculate with accuracy at the integration time step $10^{-6}s$ for the motion with the high moving velocity 300km/h. It is supposed that we have to pay attention to the integration time step, when the translation velocity is not so smaller than the propagation velocity of the wave in the beam.

Table 1 Parameters for numerical analysis

Wheel	Material		S45C
	Young's Modulus [N/m^2]	E	2.058×10^{11}
	Poisson Ratio	v	0.30
	Mass [kg]	M	10
	Radius [m]	ρ_0	0.1
Rail	Material		S45C
	Young's Modulus [Pa]	E	2.058×10^{11}
	Poisson Ratio	v	0.30
	Density [kg/m^3]	K	7850
	Length [m]	l	1.0
	Sectional Height [m]	h_1	0.02
	Sectional Width [m]	b_1	0.01
	Sectional Area [m^2]	a	6.936×10^{-3}
	Mass Moment of Inertia [m^4]	I	3.08961×10^{-5}
Others	Elastic Support [MN/m]	k_s	140
	Interval of Supports [m]	d_s	0.5
	External Force on Wheel [N]	F_w	47040

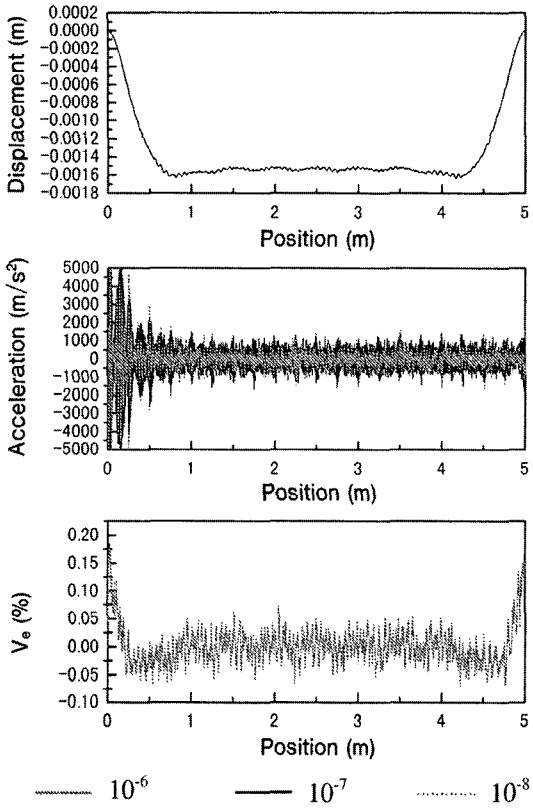

Fig. 4 Effect of integration time step

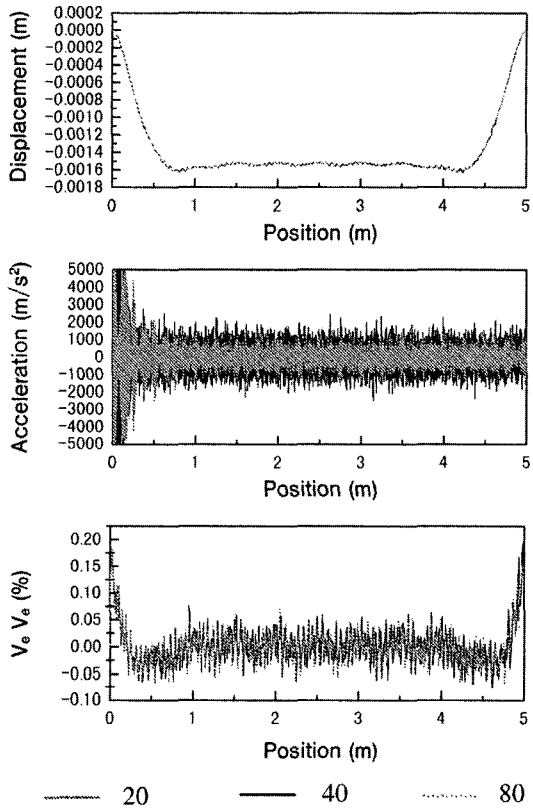

Fig. 5 Effect of elements mumber

We also investigate the reasonable number of the elements, comparing the results with 20, 40 and 80 elements. Translation velocity 200 km/h, the support elasticity 140 MN/m and the integration time step $10^{-7}s$ are given. Fig. 5 shows the numerical results for each number of elements. The calculation error and the displacement of the contact point for the number of elements 20, 40 and 80 are in good agreement quantitatively. When we consider the displacement of the contact point, optimized element number is about 20. However, we need the element number 40 for the discussion of the acceleration.

From the above discussion, we adopt the integration time step $10^{-7}s$ and the number of elements 20 or 40.

4.3 Effect of supports stiffness on displace ment at contact point

In this subsection, the interval length of the elastic supports, number of element, time unit are given as 0.5 m, 20 and $10^{-7}s$ respectively. We focus on the effect of the support elasticity on the dynamic behavior of the system.

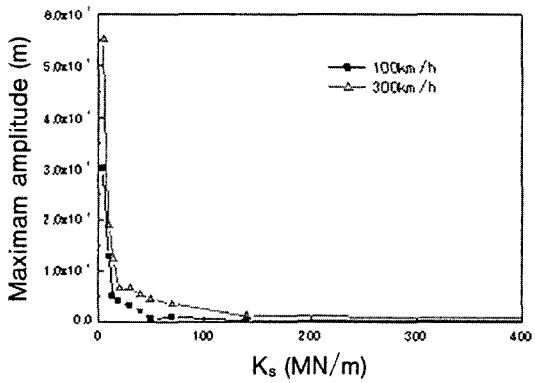

Fig. 6 Supports stiffnedd and displacement at Contact

Fig. 6 shows the maximum amplitude of the vibration at the contact point with high frequency for moving velocity 100 km/h and 300 km/h. It is

mentioned that the maximum amplitude of the displacement at the contact point shifts up on the whole with the increase of the support elasticity. The amplitude for both velocity decreases with the increase of the support elasticity. It is also noticed that the effect of the high moving velocity on the amplitude of the displacement at the contact point becomes remarkable relatively around 70-140 MN/m.

4.4 Effect of moving velocity

In this section, the influence of the moving velocity on the frequency of the system during the passage and the amplitude of the displacement at the contact point are discussed. Some moving velocities from 50 km/h to 400 km/h are given. Support elasticity 140 MN/m is also given. These investigations are summarized in Fig. 7.

The main frequency occurred during the passage does not depend on the moving velocity. On the other hand, the amplitude of the displacement at the contact point increases with the increase of the moving velocity. It is supposed that the external force with the frequency due to the passage on the elastic supports exerts on the system vibration.

In this case, it is shown that the main frequency of the displacement at the contact point is about 400 Hz and it corresponds to the third mode of the system vibration, using the eigen values shown in Fig. 3. Therefore, we can understand that the main frequency of the system vibration is almost constant for the moving velocity because the coupling effect with the contact rigidity is still strong in this mode.

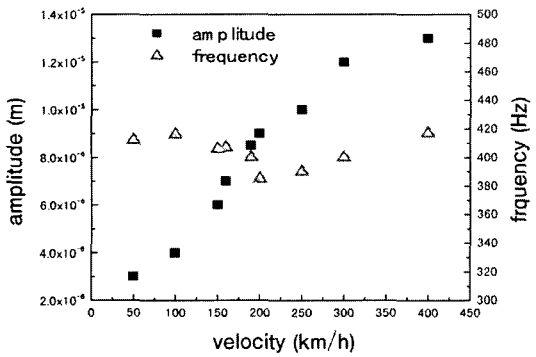

Fig. 7 Maximum amplitude and main frequency

4.5 Effective factors on acceleration at contact point

The effective factors to the acceleration at the contact point are clarified in this subsection. From a viewpoint of the multibody dynamics, the constraint condition for the unilateral contact gives the valuable information in the numerical approach. It is described with some terms including the components of the acceleration at the contact point.

In this section, we aim to point out the governing factors for the vertical vibration of the system at the contact point Because of the constant moving velocity, we can neglect the influence of the first two terms of the left hand side in Equation (21). In addition, as ϕ is small enough in

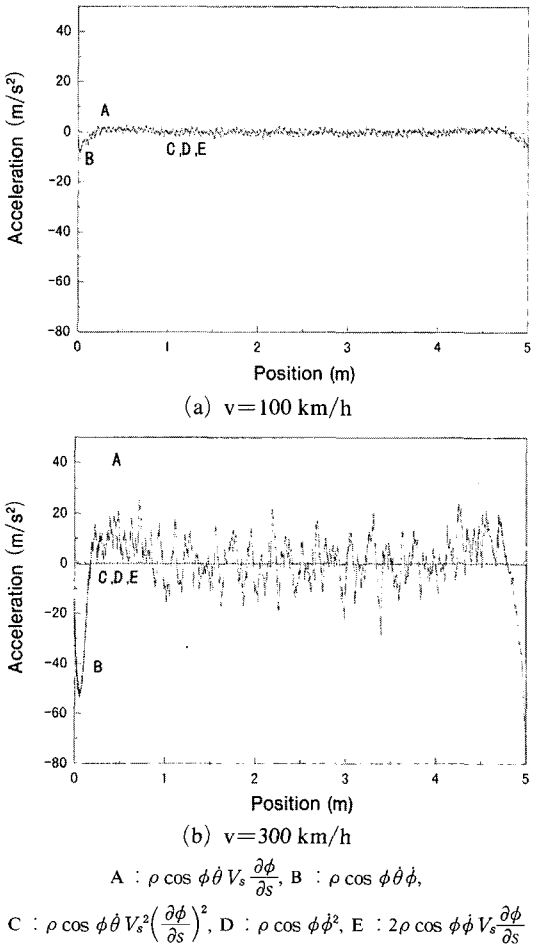

A : $\rho \cos\phi \dot{\theta} V_s \frac{\partial \phi}{\partial s}$, B : $\rho \cos\phi \dot{\theta}\dot{\phi}$,

C : $\rho \cos\phi \dot{\theta} V_s^2 \left(\frac{\partial \phi}{\partial s}\right)^2$, D : $\rho \cos\phi \dot{\phi}^2$, E : $2\rho \cos\phi \dot{\phi} V_s \frac{\partial \phi}{\partial s}$

Fig. 8 Influence of each term for acceleration

these cases, we can neglect the terms without the sixth and the seventh terms.

Fig. 8 shows the acceleration fluctuation of these terms, comparing (a) translation speed 100 km/h and (b) 300 km/h. In the results with the high speed, we can verify that the effect of the interaction among the translation and the rotation of the wheel, and the vertical vibration of the rail become remarkable. The effect is proportion to the square of the magnitude of moving velocity. These results point out that we can not neglect the effect of the incline of the rail due to its flexibility on the vertical acceleration at the contact point.

5. Conclusion

In this paper, we propose modeling and numerical simulation for the dynamic behavior of the rail/wheel system, considering high translation speed, rail elasticity, elastic supports under the rail, contact rigidity and so on. Modeling and formulation for an accurate simulation is discussed for the complex phenomena caused by the interaction between the rail and the wheel. We also discuss about the numerical approach with the finite elements. Such as the number of elements and the time step are optimized in numerical approach. Finally we attempt to verify the mechanism of the coupled vibration between the rail and the wheel, using the eigen value analysis and the constraint conditions for the unilateral contact.

It is shown that the amplitude of the lateral vibration of the rail increases with the increase of moving velocity. On the other hand, the frequency of it does not depend on the translation velocity. We can understand this property from the results of the eigen value analysis. The natural frequency of the actual vibration mode, third one, is almost constant during the passage of the wheel. These are due to the coupling between the elastic supports and the rail flexibility.

Using the unilateral contact condition, it is also clarified that the acceleration of the contact point is mainly caused by the coupling terms among the translation and the rotation of the wheel, and the vertical vibration of the flexible rail.

References

Shabana, A. A. et al., 1998, "Application of the Absolute Nodal Coordinate Formulation to Large Rotation and Large Deformation Problem," *Journal of Mechanical Design*, Vol. 120, pp. 100~106.

Takahashi, Y. and Shimizu, N., 2001, "Study on Derivation and Application of Mean Axis for Deformable Beam by Means of the Absolute Nodal Coordinate Multibody Dynamics Formulation," *Proceedings of DETC'01*, ASME Design Engineering Technical Conferences & Computers and Information in Engineering Conference, Pittsburgh U.S.A, CD-ROM.

Terumichi, Y. et al., 2001, "Dynamics of Rolling Wheel with Contact Rigidity and Slip," *Proceedings of DETC'01*, ASME Design Engineering Technical Conferences & Computers and Information in Engineering Conferences, Pittsburgh U.S.A. CD-ROM.